Journal of Saudi Chemical Society (2010) **14**, 23–31

King Saud University

Journal of Saudi Chemical Society

www.ksu.edu.sa
www.sciencedirect.com

ORIGINAL ARTICLE

Synthesis and spectroscopic, magnetic and cyclic voltammetric characterization of some metal complexes of methionine: $[(C_5H_{10}NO_2S)_2M^{II}]$; M^{II} = Mn(II), Co(II), Ni(II), Cu(II), Zn(II), Cd(II) and Hg(II)

M.A. Mamun, Omar Ahmed, P.K. Bakshi, M.Q. Ehsan *

Department of Chemistry, University of Dhaka, Dhaka-1000, Bangladesh

Received 2 February 2009; accepted 15 July 2009
Available online 16 December 2009

KEYWORDS

Synthesis;
Spectroscopic;
Cyclic voltammetric;
Complexes;
Methionine

Abstract Some metal complexes of DL–methionine were prepared in aqueous medium and characterized by different physico-chemical methods. Methionine forms 1:2 complexes with metal, M(II). The general empirical formula of the complexes is proposed as $[(C_5H_{10}NO_2S)_2M^{II}]$; where M^{II} = Mn(II), Co(II), Ni(II), Cu(II), Zn(II), Cd(II) and Hg(II). All the complexes are extremely stable in light and air and optically inactive. Magnetic susceptibility data of the complexes demonstrate that they are high spin paramagnetic complex except Zn(II), Cd(II) and Hg(II) complexes. The bonding pattern in the complexes are similar to each other as indicated by electronic absorption spectra and FTIR spectral analysis. The current potential data, peak separation (AE) and the peak current ratio (i_{pa}/i_{pc}) of the (Mn, Cu and Cd) complexes indicate that the charge transfer processes are irreversible, the systems are diffusion controlled and also adsorptive controlled. The charge transfer rate constant of metals in their complexes are less than those in their metal salts at identical experimental conditions due to the coordination of metal with methionine.

1. Introduction

Methionine is one of the sulphur containing essential amino acids. It is used as nutritional supplement and act as antioxidant in biological system. The transition metals like Mn(II), Co(II), Ni(II), Cu(II) and Zn(II) are essential trace elements and used as nutritional supplement. They act as cofactors in various enzyme systems i.e. as metalloenzymes or as enzymatic activators (Moester, 1960; Hugnes, 1981; Berg et al., 2001; Nelson and Cox, 2000). Cd and Hg are toxic elements. Methionine is a biological chelating agent may lower the

* Corresponding author.
E-mail address: mqehsan@yahoo.com (M.Q. Ehsan).

1319-6103

doi:10.1016/j.jscs.2009.12.005

Production and hosting by Elsevier

degree of toxicity for the formation of chelate with toxic metals (Dwyer and Mellor, 1964). Structure of a biologically important molecule has importance in both the pharmacy and medicine. From the clinical and biopharmacological points like efficacy, less toxicity, side effects in the treatment of different diseases, combination drugs are in great demand now a days. In the present research, the prepared essential trace metal complexes may be a combination of nutritional supplements like metal and essential amino acid; methionine may be a provider of both the micronutrients in biological system. Metal-ligand complexation improves the bioavailability increasing solubility in the gastrointestinal fluid, may lower toxicity, and may give a sustained releases product – required as medication.

The coordinating behavior of amino acid with different metal ions have been examined in our laboratory and reported in detail (Ehsan et al., 1997a,b, 1988, 1999a,b, Haider et al., 1986; Rahman et al., 2007; Ehsan et al., 1996, 1997c). In the current interest we investigated the coordination of DL–methionine with Mn (II), Co (II), Ni (II), Cu (II), Zn (II), Cd (II) and Hg (II) salts in aqueous medium and obtained metal complexes in crystalline form. Their synthesis, isolation and speciation by different analytical methods and cyclic voltammetric studies are demonstrated.

2. Experimental

2.1. Materials and methods

The chemicals and reagents used in the synthesis were of AR grade (E. Merck, BDH and Aldrich). Elemental analysis of the complexes was done at Tohoku University, Japan, and metal content was determined by AAS (Shimadzu, Japan). Water content in the complexes was determined by using a Karl Fischer Auto Titrator. FTIR spectra were recorded on an Infrared Spectrophotometer (IR-8300, Shimadzu, Japan) in the range 400–4600 cm^{-1} as KBr pellets. The electronic spectra were recorded on a UV–visible spectrophotometer (1601 PC, Shimadzu, Japan) using nujol mull as the dispersion medium. Magnetic properties were studied at ambient temperature on a Calibrated Magnetic Susceptibility Balance (Magway MSB Mkl, Sherwood Scientific Ltd, Cambridge, England). QSTG analysis was carried out by a temperature control Electric Furnace (Heraeus, FC-222, UK). The crystallinity test for all the compounds were conducted in nujol mull as dispersion medium using ZEISS digital microscope (with CARL ZEISS optical lenses), Germany. Polarimetric analysis was performed using a PC controlled calibrated Polarimeter (LC 341, Perkin Elmer, USA). Cyclic Voltammetric (CV) Studies were conducted with a PC controlled BAS Epsilon electrochemical analyzer, USA. A three-electrode electrochemical cell made of borosilicate glass and Teflon cap was used in this study. The electrodes used are Glassy Carbon Electrode (GCE) as working electrode, Ag/AgCl (Standard KCl) as reference electrode and Pt wire as counter electrode.

2.2. Preparation and formulation

The metal complexes were prepared in the aqueous medium. Two general methods (methods A and B) were fixed for the synthesis of the complexes as described below.

Method A: About 0.6–1.4 g metal salt was taken in a beaker and dilute ammonia was added. The precipitate of metal hydroxide was filtered and washed thoroughly with deionised water until the precipitate was freed from ammonia. Then the precipitate was taken in a round bottom flask. About 0.74 g methionine was taken and dissolved in 200 mL deionized water. The solution was filtered and mixed with precipitate in the round bottom flask. The mixture was refluxed for about one hour. Then the mixture was filtered with filter paper at the hot condition. The filtrate was taken in a 500 mL beaker and was evaporated to reduce the volume to about 30 mL and was kept overnight for crystallization. The crystals were separated and washed with deionized water and dried at 50 °C in a oven for about 2 h and the product was kept in a desiccator. The methionine complexes of the metals [M = Co(II), Ni(II), Cu(II), Zn(II) and Hg(II)] were prepared following this method.

Method B: About 0.74 g of methionine and about 0.265 g of Na_2CO_3 were taken in a beaker containing about 200 mL of water and were heated to dissolve the mixture. The pH of the solution was adjusted to about 7.0 and filtered. About 0.30–0.55 g of M(II) salt was dissolved in 50 mL deionized water and was filtered using filter paper. Both the filtrate was mixed together and refluxed for about 1 h. The mixture was filtered in the hot condition in a 500 mL beaker. The solution was then evaporate slowly and reduce the volume to about 30 mL and was kept overnight for crystallization after filtration. The crystals were separated and washed with deionized water and dried at 50 °C in an oven for about 2 h and the product was kept in a desiccator. The manganese and cadmium complex of methionine was prepared using this method.

The formulation of the complexes was done by comparing the experimental and calculated data for elemental analysis. The micro analytical data of C, H, N, S and M in the prepared complexes are tabulated in Table 1.

3. Results and discussion

The complexes were characterized by different physico-chemical techniques and some properties were investigated. The compounds are insoluble in most of the common solvents such as water, methanol, ethanol, DMSO etc. but soluble in dilute mineral acids and alkali. The microscopic views of particles of the complexes indicate that the crystalline nature of the complexes is different from the parent ligand and the shapes of the crystals in most of the complexes are irregular.

All the complexes melted with decomposition far below the melting point of the ligand (264 °C) owing to the formation of new compound with metal. The Karl Fischer Analysis, QSTGA and FTIR data of the complexes strongly support that crystalline or chemically coordinated water is absent in the complexes.

4. IR spectral analysis

The tentative assignments have been done on the basis of standard references and some published papers (Pavia et al., 1979; Silverstein et al., xxxx; Rao, 1963; Nakamoto, 1978). The characteristic bands of the complexes are listed in Table 2. The pattern of the IR spectra of other complexes are almost similar with each other with some exceptions. Most of the important

Table 1 The percentage of C, H, N, S and M in the complexes of methionine.

Compound	Found	%C cal.	%H found	Cal.	%N found	Cal.	Found	%S cal.	% Metal	
									Found	Cal.
$[Mn(C_5H_{10}NO_2S)_2]$ A	33.53	34.16	5.34	5.74	7.38	7.97	18.17	18.25	16.15	15.64
$[Co(C_5H_{10}NO_2S)_2]$ B	33.39	33.71	5.44	5.66	7.78	7.86	17.54	18.00	15.70	16.54
$[Ni(C_5H_{10}NO_2S)_2]$ C	32.53	33.73	5.59	5.66	7.58	7.87	18.21	18.01	16.59	16.48
$[Cu(C_5H_{10}NO_2S)_2]$ D	33.11	33.28	5.38	5.59	7.79	7.76	17.75	17.77	16.17	17.61
$[Zn(C_5H_{10}NO_2S)_2]$ E	32.81	33.11	5.36	5.56	7.71	7.72	17.60	17.68	16.86	18.02
$[Cd(C_5H_{10}NO_2S)_2]$ F	28.36	29.35	4.61	4.93	6.54	6.85	14.83	15.69	28.15	27.50
$[Hg(C_5H_{10}NO_2S)_2]$ G	23.98	24.17	3.97	4.06	5.70	5.64	12.70	12.91	41.33	40.35

Table 2 The most significant FTIR bands (cm^{-1}) of the DL–methionine and its complexes.

Comp.	ν(N–H) (str.)	ν(C–H) str. of (CH_2S)	ν(COO) (asym str.)	ν(COO) (sym str.)	ν(S–CH) (bend.)
$[Mn(C_5H_{10}NO_2S)_2]$	3340 (m–s, sp), 3267 (s,sp)	2914 (m–s, b)	1570 (s, b)	1408 (m, sp)	1257 (m-s, sp)
$[Co(C_5H_{10}NO_2S)_2]$	3346(s sp), 3275 (vs, sp)	2914 (m–s, b)	1578 (vs, sp)	1408 (s, b)	1250 (w, sh)
$[Ni(C_5H_{10}NO_2S)_2]$	3348 (s, sp), 3273 (s, sp)	2914 (s, b)	1582 (vs, b)	1408 (s, sp)	1255 (w, sh)
$[Cu(C_5H_{10}NO_2S)_2]$	3238 (s, sp), 3132 (w, sh)	2914 (m, sp)	1616 (s, sp)	1429 (w, sp)	1248 (w, sh)
$[Zn(C_5H_{10}NO_2S)_2]$	3210 (w, b), 3356 (w, b)	2916 (m, b)	1605 (s, b)	1425 (s, sp)	1242 (w, b)
$[Cd(C_5H_{10}NO_2S)_2]$	3331 (s, sp), 3252 (vs, sp)	2914 (s, sp)	1587 (s, b)	1406 (s, sp)	1283 (m, sp)
$[Hg(C_5H_{10}NO_2S)_2]$	3447 (w, b), 3208 (w, b)	2918 (w, sh)	1570 (vs, b)	1398 (s, sp)	1234 (m, sp)

s = strong, vs = very strong, str. = stretching, m = medium, w = weak, sp = sharp, sh = shoulder, b = broad.

bands in all the complexes were shifted significantly compare to that of the free ligand which indicate the formation of new compound. The intensity of bands in the complexes has been reduced in most of the cases comparing the intensity of bands found in the free ligand.

In the FTIR spectra of $[Mn(C_5H_{10}NO_2S)_2]$ (Fig. 1), there is a sharp doublet peak at 3340 and 3267 cm^{-1} which is due to asymmetric and symmetric stretching vibration of N–H in a primary amine group which demonstrate that the NH_3^+ group of zwitterions of free ligand is deprotonated to $–NH_2$ and participated in the coordination with metal ion. The bending absorption bands for NH_3^+ vibration is almost disappeared in the complex due to same reason. The band for C–H stretching vibration appears at 2915 cm^{-1} which is more sharper than that of free ligand. The $–COO^-$ asymmetric and symmetric absorption bands occur at 1570 and 1408 cm^{-1}, respectively which are at relatively lower frequencies compare to those of free ligand. The reduction of absorption frequencies may be due to the formation of coordination bond through oxygen atom of $–COO^-$ group with metal ion.

Since there is no significant absorption band at about $\nu > 3450$ cm^{-1} for ν(O–H) absorption in any of the complexes, we can conclude that there is no water molecule in the complexes as coordinated water or as water of crystallization. In Cu(II) complex a weak insignificant absorption band is observed at about 3466 cm^{-1} which may be due to the O–H stretching vibration for the presence of moisture in the sample. In Hg(II) complex all the peaks appear as weak and broad band. It may be due to the mass effect (higher atomic mass) of Hg in the complex. This higher atomic mass is the major part of the molecular weight of the complex which is responsible to lowering the intensity of chromophore in the complex molecule.

DL–methionine (ν, cm^{-1}): 3414 $\nu_{str}(NH_3^+)$, 2914 ν_{str} (C–H), 1630 $\nu_{as}(NH_3^+)$, 1580 $\nu_{as}(COO^-)$, 1516 ν_{sb} (NH_3^+), 1413 $\nu_s(COO^-)$, 1220 ν_b(S–CH).

5. UV–vis spectral analysis

The electronic absorption spectra of the methionine complexes and their characteristics absorption bands with tentative assignments are presented in Fig. 2 and Table 3, respectively. The assignments have been done on the basis of some standard references (Lang, 1961; Gillam and Strem, 1957; Jatte and Orchin, 1962).

The absorption bands between 200 and 400 nm were observed for the organic part of the complexes and that of >400 nm was due to the metal ion. The bonding pattern of the DL–methionine complexes were similar in most of the cases. The bands due to $\pi \rightarrow \pi^*$ transition in all the metal complexes at ~236–257 nm were broad. Whereas in DL–methionine it was found at about 236 nm.

The presence of the absorption band at ~295–299 nm in the complexes was due to $n \rightarrow \sigma^*$ transitions that was observed at 297 nm in ligand. The $n \rightarrow \pi^*$ transition bands were observed at 318–365 nm (at 338 and 350 nm in ligand) in almost all

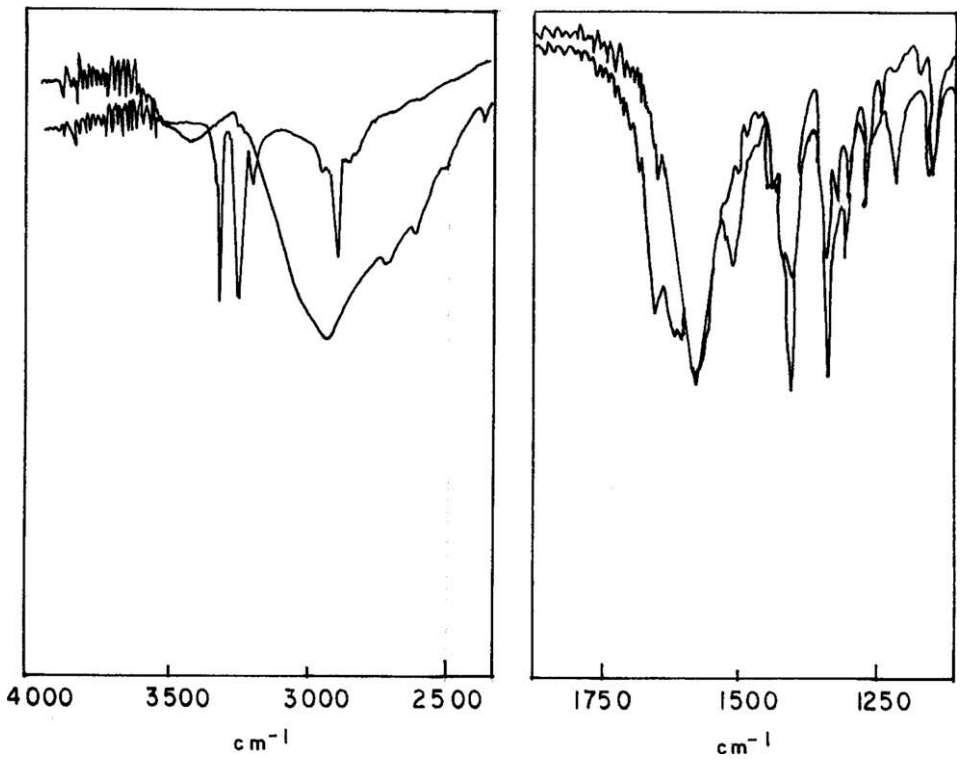

Figure 1 IR spectra of $PVIn(C_5H_{10}NO_2S)_2]$ and the ligand in the region (A) 3500–2000 cm^{-1} and (B) 1750–1250 cm^{-1}.

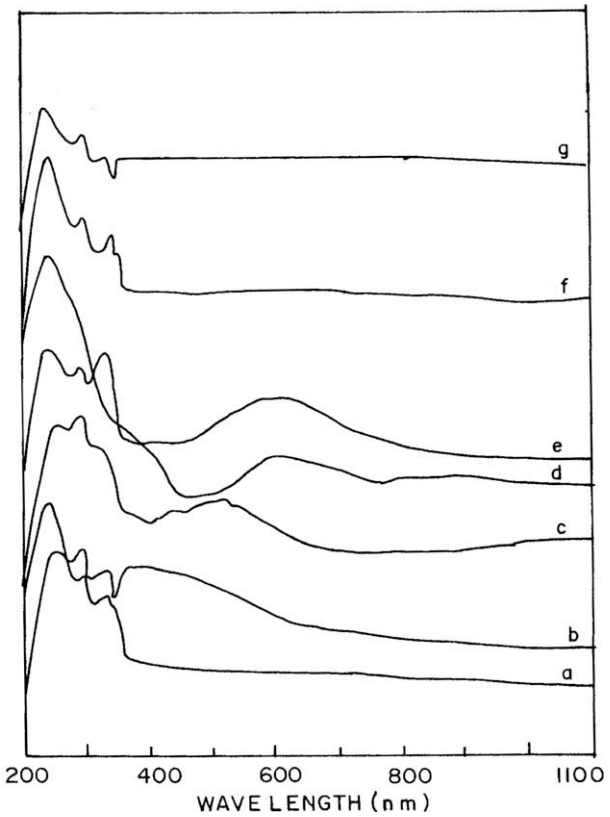

Figure 2 The UV–vis absorption spectra of (a) DL–methionine, (b) $[Mn(C_5H_{10}NO_2S)_2]$, (c) $[Co(C_5H_{10}NO_2S)_2]$, (d) $[Ni(C_5H_{10}NO_2S)_2]$, (e) $[Cu(C_5H_{10}NO_2S)_2]$, (f) $[Zn(C_5H_{10}NO_2S)_2]$ and (g) $[Cd(C_5H_{10}NO_2S)_2]$ complexes in the region 200–1100 nm.

the metal complexes. The presence of $\pi \rightarrow \pi^*$, $n \rightarrow \pi^*$ and $n \rightarrow \sigma^*$ bands in all the complexes indicate the presence of the functional groups of the parent ligands (e.g. –C═O, –NH_2 and C–S) intact in the complexes. A large shifting of the absorption bands in the complexes and appearing of a new band for d–d transitions also indicate the probability of forming $M^+ \leftarrow L$ coordination bonds in the complexes.

Transition metal complexes are generally colored and this color arises due to the absorption of light in visible region. Therefore, the broad bands centering around 413 nm in Mn(II), 520 nm in Co(II), 635 and 898 nm in Ni(II) and 664 nm in Cu(II) complexes are clearly due to the d–d electronic transitions, which causes color of the complexes.

In case of Zn(II), Cd(II) and Hg(II) complexes no absorption band for d–d transitions in the visible region are due to the fact that all are d^{10} system.

6. Magnetic properties

Magnetic moments of all the complexes were measured using a manual magnetic susceptibility balance are reported in Table 4. The measured values agree with the divalent oxidation state of the metals. The μ_{eff} values of the complexes demonstrate that all the complexes are sufficiently pure and no paramagnetic contaminations are present in the complexes. The complexes of Mn(II), Co(II), Ni(II) and Cu(II) are high spin paramagnetic as suggested by their magnetic moment values (Earnshaw, 1968; Foex et al., 1957; Selwood, 1956). The other complexes are diamagnetic as they are d^{10} system. The literature value crystal field stabilization energy (CFSE) of these types of complexes is favorable for the formation of octahedral complex. So, we suggest octahedral geometry of all the complexes.

Table 3 Absorption bands of DL–methionine and its complexes.

Compound	Appearance	Absorption bands (nm)			
		$d \rightarrow d^*$	$n \rightarrow \pi^*$	$n \rightarrow \sigma^*$	$\pi \rightarrow \pi^*$
DL–methionine	White crystalline powder	–	350, 338	297	236
$[Mn(C_5H_{10}NO_2S)_2]$	Light caramel crystalline powder	413	365, 338	299	253
$[Co(C_5H_{10}NO_2S)_2]$	Light violet crystalline powder	520	348, 332	295	256
$[Ni(C_5H_{10}NO_2S)_2]$	Sky-blue crystalline powder	635, 898	351, 335	297	243
$[Cu(C_5H_{10}NO_2S)_2]$	Blue crystalline powder	604	349, 341	296	238
$[Zn(C_5H_{10}NO_2S)_2]$	Off-white crystalline powder	–	346, 337	297	236
$[Cd(C_5H_{10}NO_2S)_2]$	White crystalline powder	–	365, 340	299	238
$[Hg(C_5H_{10}NO_2S)_2]$	Creamy white crystalline powder	–	359, 318	297	257

Table 4 Magnetic properties of the complexes of DL–methionine.

Sample ID	XA (cgs) $\times 10^3$	Jeff (BM) (at 305 K)	n = no. of unpaired electrons	Confign (m (Selwood, 1956))	Inference
$[Mn(C_5H_{10}NO_2S)_2]$	14.18	5.88	5	d^5	Paramagnetic
$[Co(C_5H_{10}NO_2S)_2]$	8.40	4.53	3	d^7	Paramagnetic
$[Ni(C_5H_{10}NO_2S)_2]$	3.563	2.95	2	d^8	Paramagnetic
$[Cu(C_5H_{10}NO_2S)_2]$	1.23	1.732	1	d^9	Paramagnetic
$[Zn(C_5H_{10}NO_2S)_2]$	Negative	*0	0	d^{10}	Diamagnetic
$[Cd(C_5H_{10}NO_2S)_2]$	Negative	*0	0	d^{10}	Diamagnetic
$[Hg(C_5H_{10}NO_2S)_2]$	Negative	*0	0	d^{10}	Diamagnetic

7. Quasi-static thermo gravimetric analysis

The QSTG analysis results of the complexes are very close to each other except the Hg(II) complex (Fig 3). The first step weight-loss is about 1.0–2.0% up to the decomposition point of each of the complexes is due to the loss of adhere surface water (%KF 0.5–1.5%) of the test specimens. This physically bound moisture was equivalent to less than 0.5 molecules of H_2O in all the complexes. Therefore this data strongly agree with the absent of any chemically bound water i.e. chemically crystalline or coordinated water in all the complexes. The second weight loss during the decomposition of the compound was (–18% to 25%) below −270 °C, this wt. loss correspond with two molecules of CO_2 due to the decomposition of two carboxyl groups present in the complex molecule.

The next weight loss (−23% to 29%) up to −350 °C may be due to the loss of two molecules of NH_3 and C–S groups (as the formation of SO_2 with air) in most of the complexes. But in Hg(II) complex this weight loss was about 34% may be due to the starting of the sublimation of Hg as HgO. The last step weight loss before attaining the constant weight at higher temperature as may be due to the removal of most of the organic part of the complexes as H_2, CH_4 and HgO gas in $[Hg(C_5H_{10}NO_2S)_2]$. The remaining weight (%) except $[Hg(C_5H_{10}NO_2S)_2]$ (where no residue was round) is in good agreement with the weight of MO(%), which is also corresponded with the percentage of MO determined by AAS and the potentiometric titration.

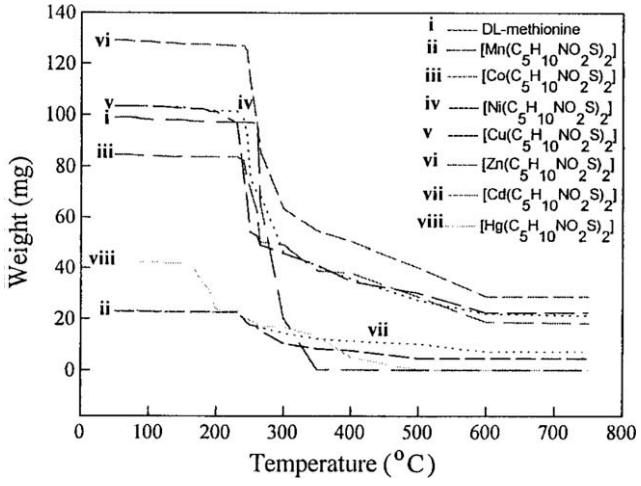

Figure 3 QSTGA curve of DL–methionine and its complexes.

8. Cyclic voltammetric studies

The redox behavior of copper, cadmium and manganese in the coordinated and uncoordinated states were examined using cyclic volatammetric technique. All the solutions in the present studies were prepared in freshly prepared chloride buffer (pH 2.2). The surface of the working electrode was polished with powdered alumina and rinsed thoroughly with deionized water before doing the experiments. The solution system was deoxygenated by purging with N_2 gas for about 30 min and was homogenized by stirring with a magnetic stirrer. The cyclic voltammograms of the solution were recorded with respect to saturated Ag/AgC1 reference electrode. In the present study, the heterogeneous charge transfer rate constant, k_f values for the electro active species were calculated from the experimental data.

8.1. CV of copper system

The redox behavior of copper in $[Cu^{II}(C_5H_{10}NO_2S)_2]$ and in copper chloride were observed on glassy carbon electrode within the potential window 1200 to −900 mV at room temperature. Cyclic voltammograms of 1 mM $[Cu^{II}(C_5H_{10}NO_2S)_2]$, ligand and metal salts are shown in Fig. 4.

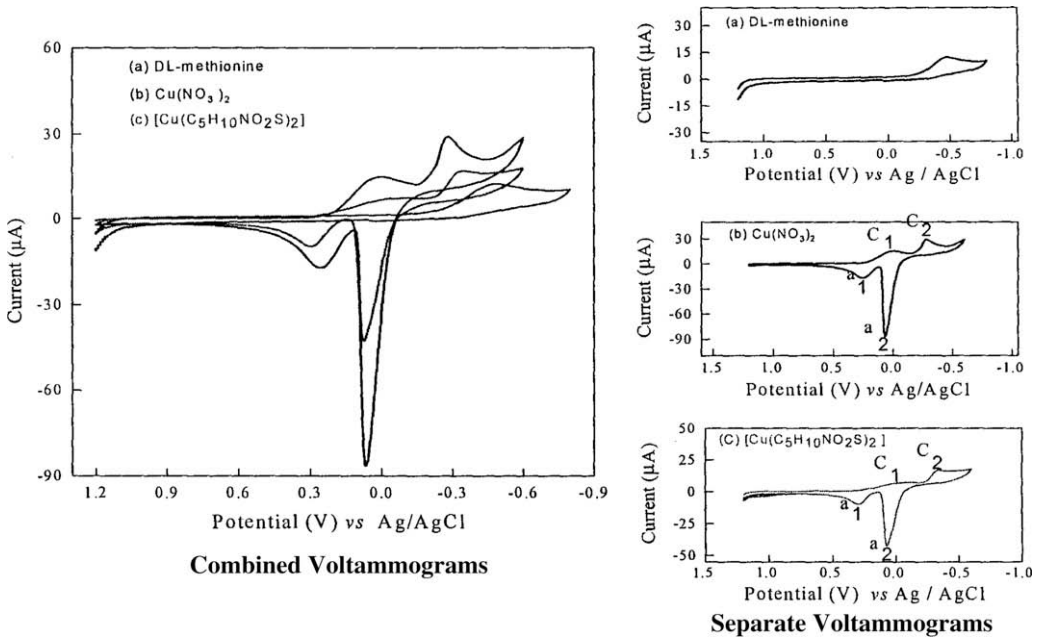

Figure 4 Cyclic voltammogram of (a) methionine, (b) Cu(II)–nitrate and (c) $[Cu(C_5H_{10}NO_2S)_2]$ in chloride buffer (pH 2.2) and their combined voltammograms on *gc* electrode vs. Ag/AgCl at scan rate 100 mVs-1.

In the metal complex (Fig. 4) there are two cathodic peaks at the potentials −0.088 and −0.339 V and two anodic peaks at 0.300 and 0.074 V, respectively. But all the peaks are broader than those in the metal salt. The positions of the cathodic and anodic peaks in the complex were shifted significantly compared to those of metal salt due to the complexation of Cu(II) with DL–methionine. The cyclic voltammograms (Fig. 4b) indicate that there are two one-electron transfer processes i.e.

cathodic reaction $Cu^{2+} \overset{+e}{\rightarrow} Cu^{+} \overset{+e}{\rightarrow} Cu^{0}$

anodic reaction $Cu^{0} \overset{-e}{\rightarrow} Cu^{+} \overset{-e}{\rightarrow} Cu^{2+}$

The current-potential data, peak separation, peak current ratio of the voltammograms at different scan rates are recorded in Table 5.

The voltammograms of this metal complex at different scan rates show the peak current of both the anodic and cathodic peaks increase with the increase of scan rate. A plot of peak current i_{pc} (μA) vs. SQRT of scan rate for the copper complex is shown in Fig. 5.

The plot shows that the i_p, value increases with the increase of scan rate *v*. A plot of cathodic peak potential, E_{pc} (vs. Ag/AgCl) vs. log *v* for metal complex (Fig. 6) express that the slope of the Tafel plot is not zero which implies that the redox process is not reversible. The plot also indicates that E_{pc} is shifted towards the positive potential with the increase of log *v*. The values of peak current ratios also demonstrate that the redox process is not reversible.

8.2. CV of cadmium system

The redox behavior of Cd(II) in Cd(II) acetate and in $[Cd(C_5H_{10}NO_2S)_2]$ were examined in chloride buffer (pH 2.2) by cyclic voltammetric technique on glassy carbon electrode at the scan rate 100 mV s^{-1} within the potential window −200 to −1000 mV at room temperature and shown in Fig. 7. In the complex the cathodic peak was observed at the

Table 5 Current-potential data, peak potential separation (AP, peak current ratio (i_{pa}/i_p of the voltammograms of 1 mM $[Cu(C_5H_{10}NO_2S)_2]$ in chloride buffer (pH 2.2) at different scan rates.

Scan rate (*v*) (V s^{-1})	Anod[c] peak potential E_{pa} (V)	Cath[c] peak potential E_{pc} V (–)	Anod[c] peak curr[f] i_{pa} A (–)	Cathd[c] peak curr[f] i_{pa1} (A)	Peak sep[n] $\Delta E = (E_{pa} - E_{pc})$ V	Peak curr[f] ratio i_{pa}/i_{pc}
0.100	0.300	0.088	9.74	7.15	0.388	1.36
0.200	0.310	0.123	13.79	10.19	0.433	1.35
0.300	0.315	0.137	16.83	12.22	0.452	1.38
0.400	0.315	0.147	19.20	14.24	0.462	1.35
0.500	0.320	0.167	21.22	15.93	0.487	1.33
2nd pair						
0.100	0.074	0.339	42.17	16.61	0.413	2.54
0.200	0.074	0.383	51.29	23.70	0.457	2.16
0.300	0.064	0.427	57.71	29.45	0.491	1.96
0.400	0.064	0.467	63.11	34.85	0.531	1.81
0.500	0.059	0.486	69.20	39.58	0.545	1.75

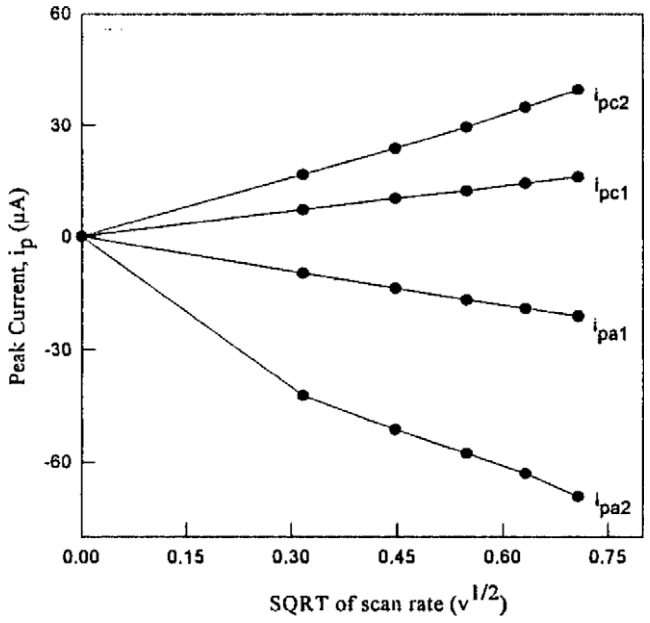

Figure 5 Variation of peak current with square root of scan rate for $[Cu(C_5H_{10}NO_2S)_2]$ in chloride buffer (pH 2.2).

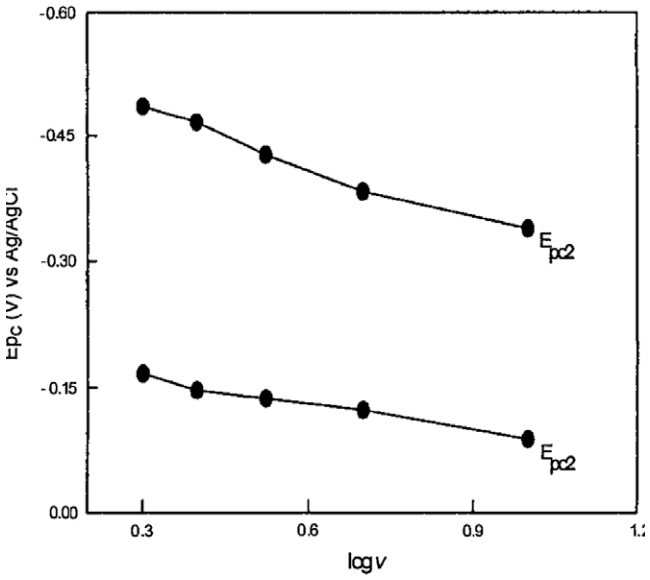

Figure 6 Effect of scan rate on peak potential of 1 mM $[Cu(C_5H_{10}NO_2S)_2]$ in chloride buffer (pH 2.2).

potential −0.784 V and the anodic peak at −0.575 V. The cyclic voltammograms of both the electroactive species indicate that there is a two electron transfer process i.e.

cathodic reaction $Cd(II) \overset{+2e}{\rightarrow} Cd^0$

anodic reaction $Cd^0 \overset{-2e}{\rightarrow} Cd(II)$

The peak current for the cathodic and anodic peak in the voltammogram of the complex is significantly lower than that of the metal salt. The cathodic peak of the complex is shifted towards the left (i.e. towards the positive potential) and the anodic peak to the right (i.e. towards the negative potential).

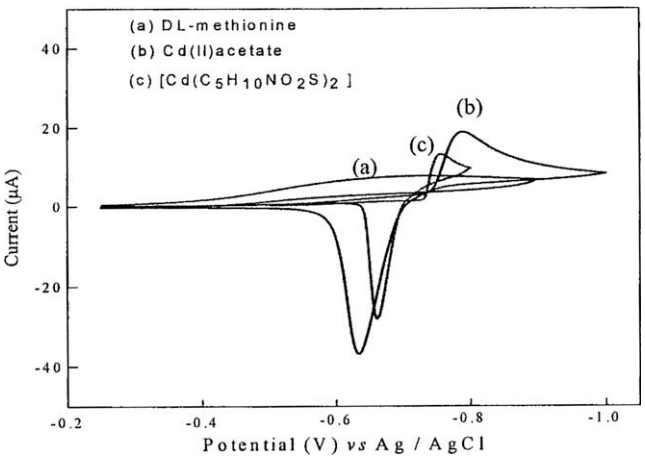

Figure 7 Cyclic voltammogram of 1 mM (a) DL–methionine, (b) Cd(II) acetate and (c) $[Cd(C_5H_{10}NO_2S)_2]$ in chloride buffer (pH 2.2) and their combined voltammograms on *gc* (glassy carbon) electrode vs. Ag/AgCl at scan rate 50 mV/s and potential window −200 mV to −1000 mV.

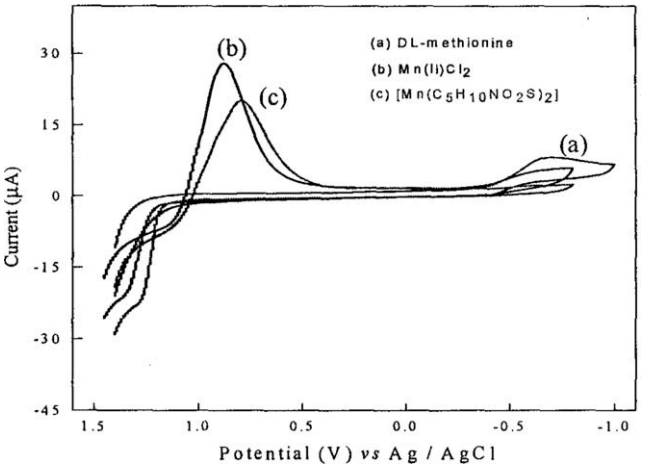

Figure 8 Cyclic voltammogram of (a) methionine, (b) $MnCl_2$ and (c) $[Mn(C_5H_{10}NO_2S)_2]$ in chloride buffer (pH 2.2) on *gc* (glassy carbon) electrode vs. Ag/AgCl at scan rate 100 mV/s and potential window 1500 mV to −1100 mV.

In the metal complex, $[Cd^{II}(C_6H_{10}N_2O_4S_2)]$ there is a cathodic peak at the potential −0.833 V and an anodic peak at about −0.605 V. The peak currents for the anodic and cathodic peak in the voltammogram of the complex is remarkably lower than that of the metal salt. Compared to the metal salt the positions of the cathodic peak in the complex has also been shifted. The plot shows the i_p value increases with the increase of SQRT of scan rate v. A plot of cathodic peak potential, E_{pc} vs. log v (Tafel plot) for metal complex express that the slope of the plot is not zero. So the electrochemical process is irreversible.

8.3. CV of manganese system

Cyclic voltammograms of 1 mM DL–methionine, 1 mM $MnCl_2$ and 1 mM $[Mn(C_5H_{10}NO_2S)_2]$ in chloride buffer

Table 6 Current-potential data, Tafel slope b, diffusion coefficient, D and the charge-transfer rate constant, kf calculated from the voltammograms of 1.0 mM metal salts and metal complexes in chloride buffer (pH 2.2) at 100 mV s^{-1} and at ambient temperature.

Sample ID	Cath^c peak poten^l E_{pc} V (–)	Cath^c peak current i_{pc} (A)	Tafel slope $b = 2.303\ RT/\alpha N_a$ (F)	Diff^n coeff. $D \times 10^{11}$ cm^{-2} s^{-1}	$-\log k_f$ (cm s^{-1})	Charge transfer rate constant $k_f \times 10^6$ (cm s^{-1})
$Cu(NO_3)_2$	0.236	23.11	0.2602	2.63	5.2832	5.21
$[Cu(C_5H_{10}NO_2S)_2]$	0.334	17.49	0.3367	1.95	5.4041	3.94
Cd(II) acetate	0.758	69.11	0.1377	12.40	4.8076	15.6
$[Cd(C_5H_{10}NO_2S)_2]$	0.805	34.28	0.0306	0.07	5.1119	7.7
$MnCl_2$	0.878	27.08	0.2372	6.58	5.0640	8.63
$[Mn(C_5H_{10}NO_2S)_2]$	0.793	17.97	0.2295	28.05	5.242	5.73

T = 298 K, n = no. of electron transferred = 2, R = 8.314 J K^{-1} mol^{-1}, F = 96,500 C, A = surface area of the electrode = 0.05 cm^2.

(pH 2.2) and their combined voltammograms are shown in Fig. 8. In the metal complex there is a cathodic peak at 0.793 V and an anodic peak at 1.280 V. The cyclic voltammograms of these electroactive species indicate that the electron transfer process is a one step process.

cathodic reaction $Mn(II) \overset{+2e^-}{\rightarrow} Mn^0$

anodic reaction $Mn^0 \overset{-2e^-}{\rightarrow} Mn(II)$

The peak currents for the cathodic peak in the voltammogram of the complex is remarkably lower than that of the metal salt.

The voltammograms of this metal complex at different scan rates show the peak current of both the anodic and cathodic peaks increase with the increase of scan rate. The 1st cathodic peaks are shifted towards right. The ΔE increases with the increase of scan rate. A plot of peak current i_{pc} (μA) vs. SQRT of scan rate (Randless–Sevcick plot) for the metal complex shows the i_{pc} value increases with the increase of SQRT of scan rate, v. A plot of cathodic peak potential, E_p vs. log v (Tafel Plot) for metal complex express that the slope of the plot is not zero. Therefore, the electrochemical process is irreversible for this system.

To calculate the heterogeneous charge transfer rate constant, k_f the current – potential data obtained from the cyclic voltammograms of metal salts and metal complexes at 100 mV s^{-1} and 200 mV s^{-1} are used.

The current-potential data, Tafel slope, diffusion coefficient and charge transfer rate constants at room temperature for metal salts and metal complexes are listed in Table 6.

Searching the redox behavior of Cu(II), Cd(II) and Mn(II) in their methionine complexes we see that the positions of the cathodic and anodic peaks in the voltammograms of all the complexes were shifted significantly compare to the metal salt due to the complexation of metal with methionine. A very high peak separation potential for the metal complex system confirm that the system is not a reversible system. The ratio of the anodic and cathodic peak currents for the electro active species are quite deviated from the unity, which also agree with the irreversibility of the system (David and Gosser, 1993). The peak heights of cathodic and anodic signals increases progressively with scan rate for these electrochemical systems supporting the process to be diffusion controlled (Bard and Faulkner, 1980). The linearity of the peak currents with the square root of scan rates represent that the electrode process is adsorptive controlled (Zhang, 1972). The kf value for metal complex system is lower than the metal salt system at an identical experimental conditions indicating the formation of $[Mn(C_5H_{10}NO_2S)_2]$ complex with methionine. The charge transfer rate constant, k_f, for metal complexes are lower than the respective metal salt at an identical experimental conditions.

Acknowledgement

Thanks are due to ministry of Science and Technology, Govt. of Bangladesh for their financial support in this work.

References

Bard, A.J., Faulkner, L.R., 1980. Electrochemical Methods. Fundamentals and Applications. John Wiley and Sons, New York, p. 228.
Berg, J.M., Tymoczko, J.L., Stryer, L., 2001. Biochemistry, fifth ed. W.H. Freeman and Company, New York, p. 41.
David, K., Gosser Jr., 1993. Cyclic Voltammetry, Simulation and Analysis of Reaction Mechanisms. Wiley-VCH, New York.
Dwyer, F.P., Mellor, D.P., 1964. Chelating Agents and Metal Chelates. Academic Press, New York and London, pp. 343, 387.
Earnshaw, A., 1968. Introduction of Magnetochemistry. Academic Press, London.
Ehsan, M.Q., Haider, S.Z., Malik, K.M.A., Khan, M.S., Quddus, R.J., 1988. Dhaka Univ. Stud. 35 (2), 153–160.
Ehsan, M.Q., Malik, K.M.A., Haider, S.Z., 1996. J. Bangladesh Acad. Sci. 20 (2), 175–181.
Ehsan, M.Q., Jebin, M., Quyser, M.A., Ahmed, E., Malik, K.M.A., Haider, S.Z., 1997a. J. Bangladesh Chem. Soc. 10 (1), 31–37.
Ehsan, M.Q., Arifur Rahman, J.M., Quyser, M.A., 1997b. J. Bangladesh Chem. Soc. 10 (2), 187–193.
Ehsan, M.Q., Rudaba, A., Quyser, M.A., 1997c. J. Bangladesh Chem. Soc. 10 (2), 195–200.
Ehsan, M.Q., Jebin, M., Quyser, M.A., 1999a. Ind. J. Chem. 38A, pp. 826–818.
Ehsan, M.Q., Rahman, J.M.A., Quyser, M.A., 1999b. J. Bangladesh Chem. Soc. 12 (1), 75–81.
Foex, G., Coiter, G., 1957. J. Constantes Selectionnees 7, Diamagnetisme et Paramagnetisme, Masson, Paris, A Collection of Diamagnetic and Paramagnetic Susceptibilities.
Gillam, Strem, E.S., 1957. An Introduction to Electronic Absorption Spectroscopy in Organic Chemistry. Arnold, London.
Haider, S.Z., Malik, K.M.A., Ehsan, M.Q., Bakshi, P.K., Khan, M.S., 1986. J. Bangladesh Acad. Sci. 10 (1), 82–92.
Hugnes, M.N., 1981. The Inorganic Chemistry of Biological Processes. John Wiley and Sons, New York.
Jatte, H.H., Orchin, M., 1962. Theory and Applications of Ultraviolet Spectroscopy. John Wiley and Sons, New York.

Lang, L., 1961. Absorption Spectra in the Ultraviolet and Visible Region. Academic Press, New York.

Moester, A., 1960, second ed. In: Biochemistry of the Amino Acids, vol. 1 Academic Press Inc., New York, pp. 19–21.

Nakamoto, K., 1978. IR and Raman Spectra of Inorganic and Coordination Compounds. third ed. John Wiley and Sons, NY, p. 211.

Nelson, D.L., Cox, Michael M., 2000. Lehninger Principles of Biochemistry, third ed. Macmillan Worth Publishers, New York.

Pavia, D.L., Lampman, G.M., Kriz, G.S., 1979. Introduction to Spectroscopy. Saunder College Publisher, USA.

Rahman, M.S., Nasim Akter, H.M., Bakshi, P.K., Ehsan, M.Q., 2007. J. Saudi Chem. Soc. 11 (2), 277–286.

Rao, C.N.R., 1963. Chemical Applications of IR Spectroscopy. Academic Press, NY, p. 364.

Selwood, P.W., 1956. Magnetochemistry, second ed. Interscience, New York.

Silverstein, M.R., Bassler, C.G., Moril, C.T., Spectroscopic Introduction of Organic Compounds, fourth ed. pp. 95–l35.

Zhang, J., 1972. J. Electroanal. Chem. 331, 945.